ELSEVIER

Polymer 42 (2001) 6747–6757

polymer

www.elsevier.nl/locate/polymer

Vibrational spectroscopic study on the photo-induced solid-state reactions of a series of muconate diesters with various side groups

Kohji Tashiro[a,*], Shinsuke Nakamoto[a], Seishi Saragai[a], Akikazu Matsumoto[b], Takashi Tsubouchi[b]

[a]*Department of Macromolecular Science, Graduate School of Science, Osaka University, Toyonaka, Osaka 560-0043, Japan*
[b]*Department of Applied Chemistry, Faculty of Engineering, Osaka City University, Sugimoto, Osaka 558-8585, Japan*

Received 15 November 2000; received in revised form 1 December 2000; accepted 5 December 2000

Abstract

In order to clarify the photo-induced solid-state reactions of a series of dialkyl *Z,Z*-muconates, the time-resolved FT–IR measurements were performed. From the observations of the IR spectral changes in these reactions, the following three types of reactions were found: (1) the polymerization reaction to give the stereoregular polymer; (2) the isomerization reaction from *Z,Z* to *E,E*-form followed by the polymerization; and (3) the polymerization to give the amorphous polymer. By the quantitative analysis of the FT–IR data, the reaction rates were evaluated for these three types of reaction. The reactivity was compared among the various kinds of muconate diesters on the basis of the packing mode of the monomers in the crystal lattice. © 2001 Elsevier Science Ltd. All rights reserved.

Keywords: Photo-induced solid-state polymerization; Muconate diester; Reaction kinetics

1. Introduction

Photo-induced solid-state reactions of organic substances have attracted much attentions owing to their unique behavior. For example, highly stereoregular polymers can be produced without any complex catalyst. In some cases a reaction from single crystal to single crystal is observed without any loss of lattice symmetry. In some other cases, however, a product is not always a single crystal but an aggregation of crystalline domains with different orientations or amorphous materials. These reactions are said to be controlled by the packing geometry of the reacting molecules in the crystal lattice, and are often described as the topochemical reaction [1–3].

Schmidt et al. found that certain cinnamic acids dimerize in the solid state by photo irradiation [4–6]. The reactivity was found to depend on the distance between the reactive double bonds of the adjacent molecules. They also observed that *Z*-cinnamic acids undergo *Z–E* isomerization reaction instead of dimerization. From these studies, the packing geometry of the molecules in the crystal lattice was found to be critical to the nature of the reaction as well as the chemical structure of the product. The photo-induced polymerization reactions were reported in many investigations. Trioxane and tetraoxane crystals, for example, change to polyoxymethylene crystal by γ-ray irradiation at an elevated temperature [7,8]. The 2,5-distyrylpyrazine was found also to experience the topochemical polymerization to yield the polymer product with the lattice symmetry kept unchanged before and after the reaction [9–11]. Another example is the solid-state polymerization of diacetylene derivatives induced by X-ray irradiation or thermal treatment [12–14]. In this case also, the symmetry of the crystal is preserved before and after the reaction. These two cases may be assumed as the examples of topotactic reactions, a special case of topochemical reactions. As a result, polymers with high stereoregularity are obtained, establishing the new field of controlled polymerization. Similar polymerization reaction was reported to occur for S_2N_2 [15] and NiX_2 $[P(CH_2CH_2CN)_3]_2$ [16].

Recently another topotactic polymerization reaction was found by Matsumoto et al. for diethyl *Z,Z*-muconate [diethyl (*Z,Z*)-2,4-hexadienedioate, EMU] [17]. Alkylammonium (*Z,Z*)-muconate also shows a polymerization reaction in the crystalline state under photoirradiation [18–20]. Upon irradiation using γ-rays, X-ray beam and even ultraviolet light, monomer crystals undergo rapid polymerization reaction to give highly stereoregular polymer crystals of ultra-high molecular weight [21–23]. The structural change

* Corresponding author. Tel.: +81-6-6850-5455; fax: +81-6-6850-5455.
E-mail address: ktashiro@chem.sci.osaka-u.ac.jp (K. Tashiro).

PII: S0032-3861(01)00014-3

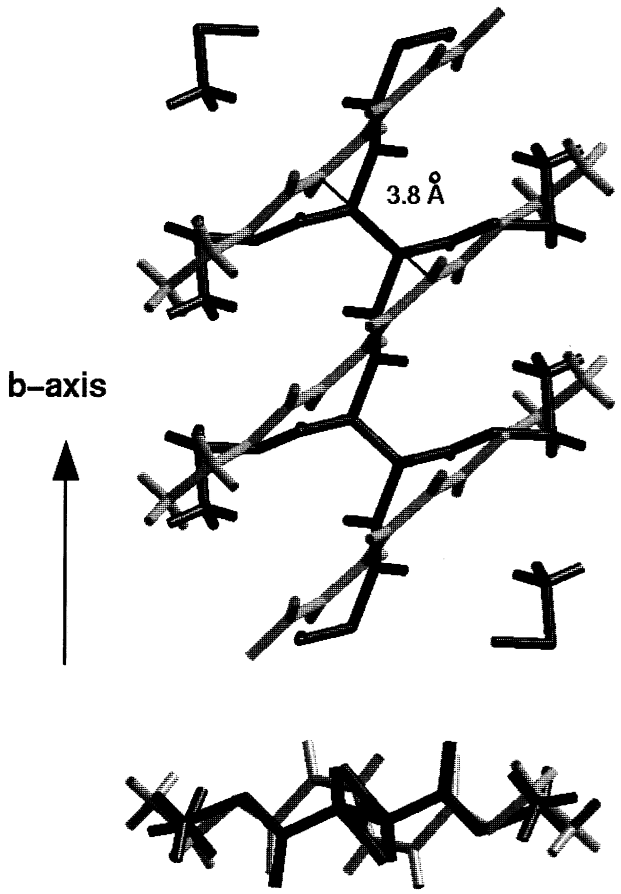

Fig. 1. Crystal structure of diethyl *Z,Z*-muconate compared between the monomer and the polymer [25].

in the single crystal-to-single crystal reaction of EMU was investigated by the time-resolved measurements of X-ray diffraction, IR and Raman spectra, and by thermal analysis, giving valuable information on the reaction kinetics, changes in the lattice parameter in the reaction process, etc. [24]. After this preliminary study, the time-resolved X-ray structural analysis was made successfully for a single crystal by utilizing the rapid-scan-type X-ray CCD camera system [25]. By this technique, the structure of the initial monomer crystal and its change with time were revealed at the atomic level. Fig. 1 shows the structural relation between the monomer and polymer. The monomer molecules form the columnar structure along the b axis. The distance between the butadiene carbon atoms of the neighboring molecules along this columnar axis is about 3.8 Å. We may speculate that the polymerization occurs smoothly and rapidly by making covalent bonds between these butadiene carbon atoms without any loss of space group symmetry. The space group of the monomer and the polymer crystals is commonly $P2_1/c$. That is to say, EMU is also an example of a topotactic polymerization reaction.

Matsumoto et al. synthesized a series of *Z,Z*-dialkyl muconates with various types of side groups and investigated their reaction behavior in the solid state [26,27]. Depending on the type of the side group, the reaction mode was found to be quite different, although the details are not yet revealed very well. In order to clarify the relationship between the reactivity and the packing structure of the monomer crystals, we carried out the crystal structure analysis of the initial monomers by the X-ray method [25,28]. Fig. 2 shows some examples of the packing structure of muconate molecules with the various side groups. Roughly speaking, the structure is similar to that of EMU, but the reaction behavior is appreciably different. We were challenged to carry out the time-resolved measurements for the single crystals of these samples, but the diffraction patterns changed only slightly. Except for the case of above-mentioned *Z,Z*-EMU single crystal, the reactions appeared to occur only at the surfaces of the single crystals, making it difficult to trace the structural changes in the photo-induced reactions. In contrast, the fine powder samples were found to react quite smoothly. Therefore, we utilized infrared spectroscopic techniques to learn the details of the reaction modes for the various types of muconate samples as will be described in the present paper. In particular, the time-resolved infrared spectral measurements were carried out and the reaction kinetics were analyzed through the quantitative analysis of the spectral data. Based on the thus-revealed information, the relation between the reactivity and the packing of the initial monomer molecules will be discussed.

2. Experimental section

2.1. Samples

The *Z,Z*-muconates used in this study are listed in Table 1. They were synthesized from (*Z,Z*)-2,4-hexadienedioic acid by methods described in Ref. [19]. The single crystals were grown by the evaporation method from the solutions. The solvents used are listed in Table 1. The thus obtained single crystals were used for the X-ray diffraction measurements and also for the IR measurements in the form of KBr disks.

Table 1
Series of muconic acid ester derivatives ROCO–CH=CH–CH=CH–COOR used in the present study and the solvents used for preparation of single crystals

Side group R	Butadiene configuration	Solvent
-CH_2CH_3	*Z,Z*	hexane
	E,E	methanol
-cyclohexyl	*Z,Z*	hexane
-benzyl	*Z,Z*	hexane
	E,E	hexane
-*n*-C_8H_{17}	*Z,Z*	acetone
-CH_2CF_3	*Z,Z*	benzene
-CH_2CCl_3	*Z,Z*	toluene

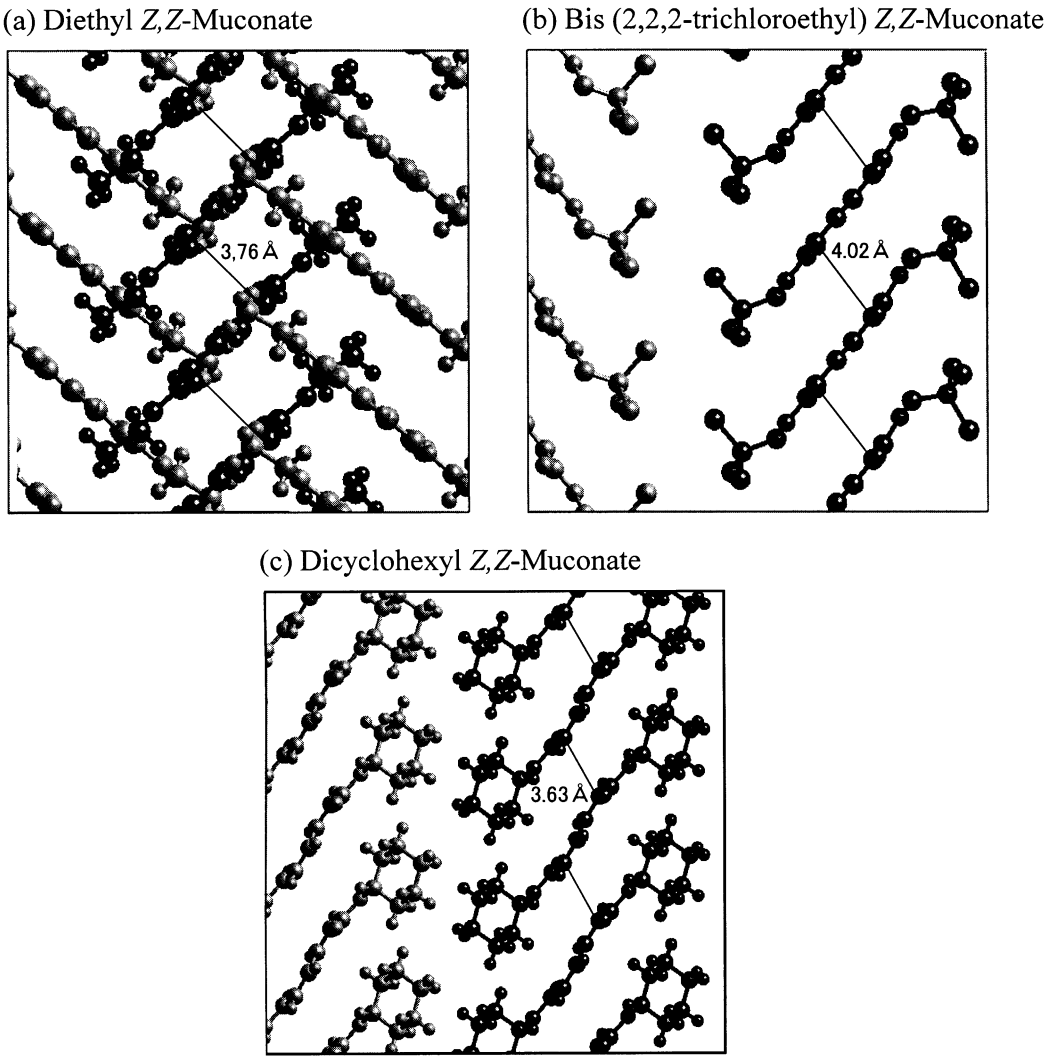

Fig. 2. Comparison of the columnar structure between the various muconate compounds. (a) diethyl *Z,Z*-muconate, (b) bis-2,2,2-trichloroethyl *Z,Z*-muconate, and (c) biscyclohexyl *Z,Z*-muconate.

2.2. Measurements

In order to analyze the IR data quantitatively with a purpose to compare the reaction rates among the various samples, the experimental conditions were adjusted exactly. The preparation condition of the KBr disk was unified by adding 3 μmol of the sample into the 250 mg of KBr powder. The infrared spectra were measured with a Bio-Rad FTS-60A/896 FT-IR spectrophotometer. The KBr disk was irradiated by a UV light repeatedly for the predetermined constant time, and then the IR measurement was performed at each time. Unfiltered medium-pressured Hg lamp was used as UV light source, where the emission power was kept constant during the measurement. The setting position of the sample was fixed tightly in front of the Hg lamp. All the procedures including the sample preparation and the spectral measurement were made in a dark room under a weak red lamp at room temperature.

3. Results and discussion

3.1. Infrared spectral changes

The infrared spectral changes are shown in Fig. 3 for the diethyl *Z,Z*-muconates in the frequency region of 1800–400 cm^{-1}. The intensity of the C=O stretching band [ν(C=O)] of the monomer at 1710 cm^{-1} decreased and the ν(C=O) band of the polymer at 1730 cm^{-1} increased in intensity as the irradiation time increased. The band at 1580 cm^{-1}, assigned to the stretching of the C=C bond [ν(C=C)] of the butadiene groups, also reduced in intensity upon irradiation by UV light and disappeared finally in the polymer spectra.

In the case of dicyclohexyl *Z,Z*-muconate, the change is more complicated as shown in Fig. 4. As the irradiation time was increased, the 1711 cm^{-1} ν(C=O) band of the *Z,Z*-monomer decreased in intensity. At the same time the

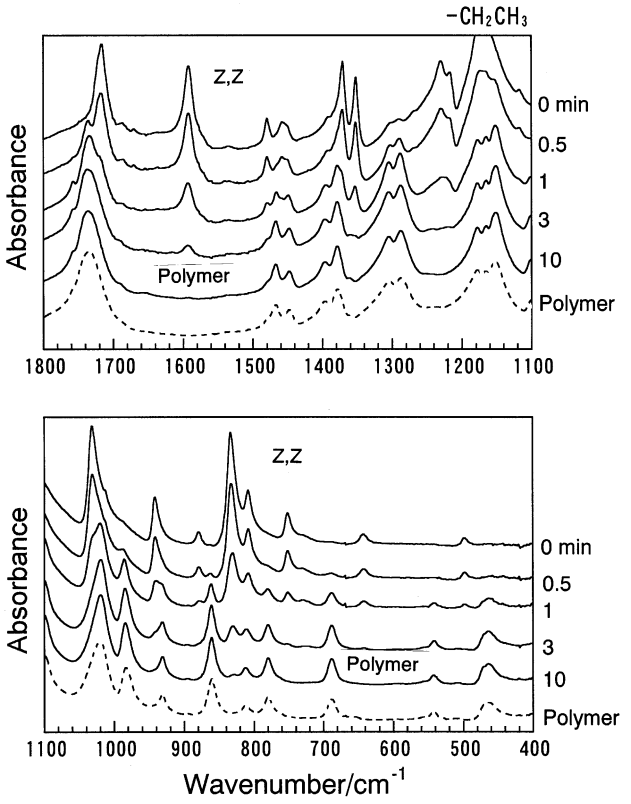

Fig. 3. UV irradiation time dependence of infrared spectra measured for diethyl *Z,Z*-muconate sample at room temperature. The spectrum shown at the bottom of each figure is of the stereoregular polymer produced from the monomer by irradiation of γ-ray for a long time.

new band appeared at 1705 cm^{-1} and increased in intensity. The spectrum was found to be similar to that of the separately synthesized *E,E*-monomer as shown at the bottom of this figure. The intensity of the *E,E*-monomer bands increased and the original *Z,Z*-monomer bands disappeared. With further irradiation, the *E,E*-species decreased in intensity and the new bands began to be observed to increase in intensity. The newly observed bands were found to correspond to those of atactic polymer as shown in Fig. 5, except for the bands at 1200 and 660 cm^{-1} which are not identified at this point. Therefore, in the case of dicyclohexyl muconate, the following reactions are considered to occur mainly: *Z,Z*-monomer → *E,E*-monomer → atactic polymer. Similar behavior was also observed in dibenzyl *Z,Z*-muconate and bis(2,2,2-trifluoroethyl) *Z,Z*-muconate.

In the case of bis-*n*-octyl *Z,Z*-muconate, as shown in Fig. 6, the bands of *Z,Z*-species disappeared upon photo-irradiation and the bands of atactic polymer appeared instead. That is, the following reaction was found to occur: *Z,Z*-monomer → atactic polymer. The same behavior was observed for bis(2,2,2-trichloroethyl) *Z,Z*-muconate.

In this way the solid-state reactions of *Z,Z*-muconates may be classified into three types as summarized in Table 2.

Table 2
The solid-state reaction paths of various muconate esters by UV irradiation

Side group R	Reaction path
$-CH_2CH_3$	*Z,Z*-isomer → tritactic polymer
cyclohexyl	*Z,Z*-isomer → *E,E*-isomer → atactic polymer
benzyl	*Z,Z*-isomer → *E,E*-isomer → atactic polymer
$-CH_2CF_3$	*Z,Z*-isomer → *E,E*-isomer → atactic polymer
$-n-C_8H_{17}$	*Z,Z*-isomer → atactic polymer
$-CH_2CCl_3$	*Z,Z*-isomer → atactic polymer

3.2. Quantitative analysis of FTIR data

3.2.1. Z,Z-monomer → tritactic polymer

Diethyl *Z,Z*-muconate undergoes a polymerization reaction upon an irradiation of light. In a series of time-dependent infrared spectra, isobestic points were observed, indicating that the reaction system may be described as a two-component system. According to Lambert–Beer's law, the infrared absorbance and molar fraction of monomer and polymer are related by the following equations.

$$I_{mono} = \epsilon_{mono} c_{mono} d \quad (1)$$

$$I_{poly} = \epsilon_{poly} c_{poly} d \quad (2)$$

$$c_{mono} + c_{poly} = 1 \quad (3)$$

where I_i, ϵ_i and c_i are, respectively, the absorbance, the molar extinction coefficient and the molar fraction of the i-th species (i = monomer or polymer) and d is the sample thickness. From Eqs. (1)–(3), we have the following equation.

$$I_{mono} = -(\epsilon_{mono}/\epsilon_{poly}) I_{poly} + d\epsilon_{mono} \quad (4)$$

This equation indicates that the plot of I_{mono} against I_{poly} should give a straight line whose slope corresponds to $\epsilon_{mono}/\epsilon_{poly}$. Combining Eqs. (1)–(3), the molar fraction of the monomer c_{mono} can be evaluated as follows:

$$c_{mono} = 1/[1 + (I_{poly}/I_{mono})(\epsilon_{mono}/\epsilon_{poly})] \quad (5)$$

The intensity I_{mono} of the EMU monomer band at 1594 cm^{-1} and I_{poly} of the polymer band at 861 cm^{-1} were plotted against time as shown in Fig. 7(a). A plot of I_{mono} versus I_{poly} is shown in Fig. 7(b). From the slope of this straight line the ratio of $\epsilon_{mono}/\epsilon_{poly}$ in Eq. (4) is obtained. By using this ratio, the time dependence of the molar fractions of monomer and polymer are evaluated as shown in Fig. 7(c).

3.2.2. Z,Z-monomer → atactic polymer

In the case of bis-*n*-octyl and bis(2,2,2-trichloroethyl) *Z,Z*-muconates, the initial monomer changes almost directly to the atactic polymer by photo-irradiation. Therefore the reaction may be treated as a two-component system. The analytical process is essentially the same as the case (1)

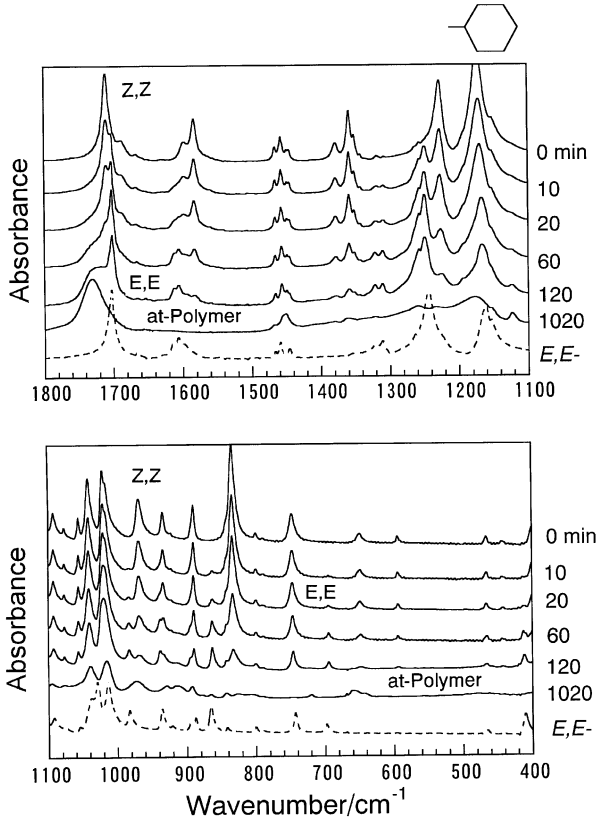

Fig. 4. UV irradiation time dependence of infrared spectra measured for dicyclohexyl *Z,Z*-muconate sample at room temperature. The spectrum shown at the bottom of each figure is of *E,E*-species synthesized separately.

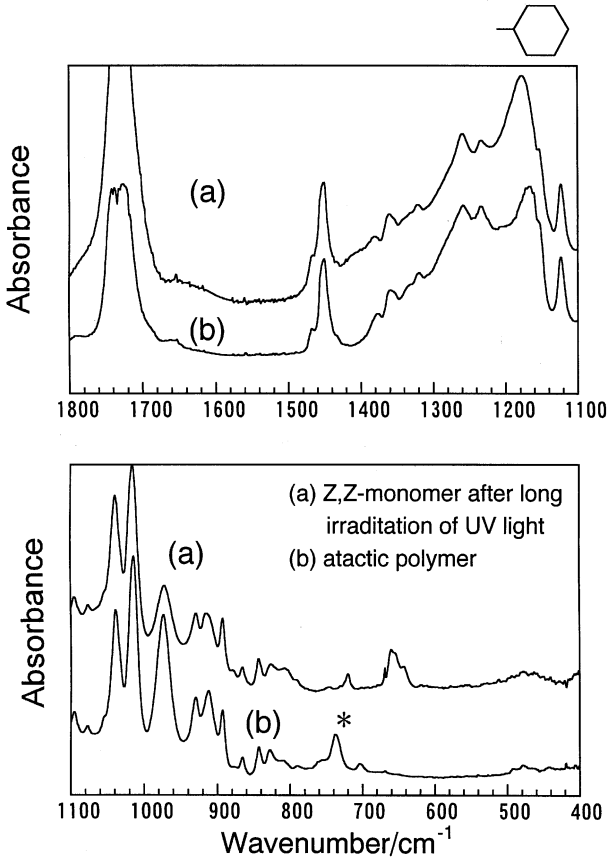

Fig. 5. Comparison of the infrared spectra of dicyclohexyl *Z,Z*-muconate between the polymer obtained after long time irradiation of UV light onto the *Z,Z*-monomer and the atactic polymer synthesized by radical reaction in the solution.

mentioned above. The time dependence of the molar fractions of monomer and atactic polymer of bis-*n*-octyl *Z,Z*-muconate is shown in Fig. 8.

3.2.3. *Z,Z-isomer → E,E-isomer → atactic polymer*

In the case of dibenzyl, dicyclohexyl and bis(2,2,2-trifluoroethyl) *Z,Z*-muconates, the reaction consists of two steps: isomerization and polymerization processes. Therefore three components coexist during the reaction, making the quantitative analysis difficult. We divided the reaction processes into the following several stages.

3.3. Initial stage of reaction

The first stage can be assumed to be the reaction system from the *Z,Z*- to *E,E*-isomer. This is acceptable as seen in Figs. 4 and 9(a), where only the bands of *Z,Z*- and *E,E*-monomer species can be observed in an early stage of reaction. The molar fraction of each monomer species can be evaluated by the method mentioned above. For the pair of the bands at 1710 cm^{-1} (*Z,Z*) and 1702 cm^{-1} (*E,E*), the ratio $\epsilon_{ZZ}/\epsilon_{EE}$ was 1.31, where the integrated intensities were used after these overlapping bands were deconvoluted by curve separation method.

3.4. Middle and later stages of reaction

In the time region later than 10 min, the system consists of three components: *Z,Z*-monomer, *E,E*-monomer and atactic polymer.

$$c_{ZZ} + c_{EE} + c_{\text{poly}} = 1 \tag{6}$$

where c_{ZZ}, c_{EE}, and c_{poly} are the molar fractions of *Z,Z*-monomer, *E,E*-monomer and atactic polymer, respectively. Combining c_{ZZ} and c_{EE} as c_{mono} or the concentration of the monomer, we have

$$c_{\text{mono}} + c_{\text{poly}} = 1 \tag{7}$$

$$c_{\text{mono}} = c_{ZZ} + c_{EE} \tag{8}$$

By using the Lambert–Beer's law in Eq. (8), we have the following relation.

$$I_{\text{mono}}/\epsilon_{\text{mono}} = I_{ZZ}/\epsilon_{ZZ} + I_{EE}/\epsilon_{EE} \tag{9}$$

By substituting ϵ_{mono} as $\epsilon_{\text{mono}} = q\epsilon_{ZZ}$, the absorbance I_{mono}

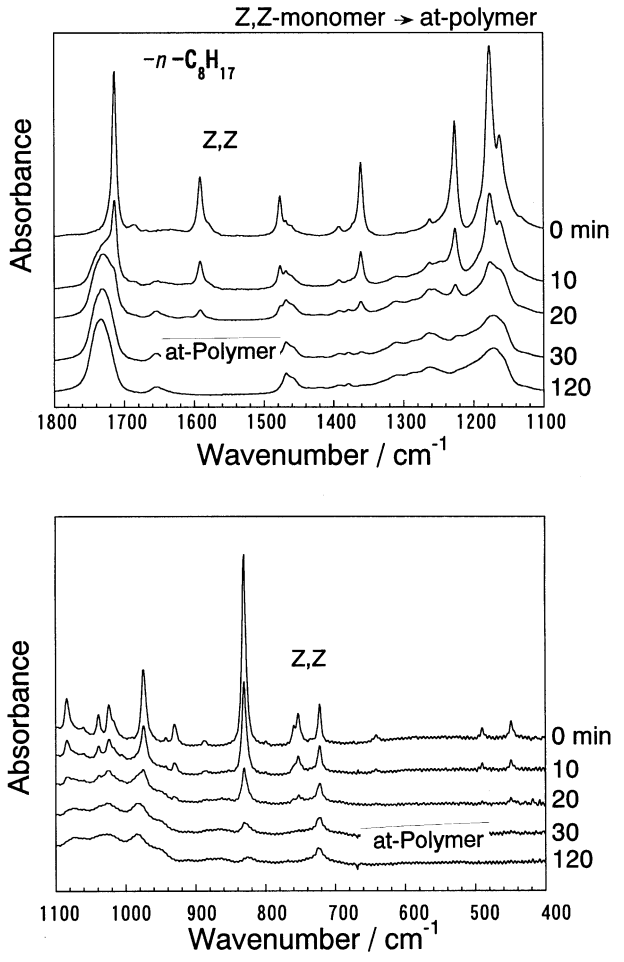

Fig. 6. UV irradiation time dependence of infrared spectra measured for bis-*n*-octyl *Z,Z*-muconate sample at room temperature.

may be expressed as follows

$$I_{\text{mono}} = (\epsilon_{\text{mono}}/\epsilon_{ZZ})[I_{ZZ} + (\epsilon_{ZZ}/\epsilon_{EE})I_{EE}]$$

$$= q[I_{ZZ} + (\epsilon_{ZZ}/\epsilon_{EE})I_{EE}] \quad (10)$$

The value 1.31, as evaluated from the infrared data for the initial stage of the reaction, is used for $\epsilon_{ZZ}/\epsilon_{EE}$ in Eq. (10). Therefore, by combining the contribution from the *Z,Z*- and *E,E*-species as the monomer, the whole system may be assumed as a two-component system consisting of the monomer and the polymer species. Thus the above-mentioned analysis can be applied to this case also. Similarly to Eq. (4), we have

$$I_{\text{mono}} = -(\epsilon_{\text{mono}}/\epsilon_{\text{poly}})I_{\text{poly}} + d\epsilon_{\text{mono}} \quad (11)$$

By using Eq. (10),

$$I_{ZZ} + (\epsilon_{ZZ}/\epsilon_{EE})I_{EE} = -(\epsilon_{\text{mono}}/q\epsilon_{\text{poly}})I_{\text{poly}} + d\epsilon_{\text{mono}}$$

$$= -(\epsilon_{ZZ}/\epsilon_{\text{poly}})I_{\text{poly}} + dq\epsilon_{ZZ} \quad (12)$$

That is to say, a plot of $I_{ZZ} + (\epsilon_{ZZ}/\epsilon_{EE})I_{EE}$ against I_{poly} gives a slope of $-(\epsilon_{ZZ}/\epsilon_{\text{poly}})$, from which the c_{mono} can be

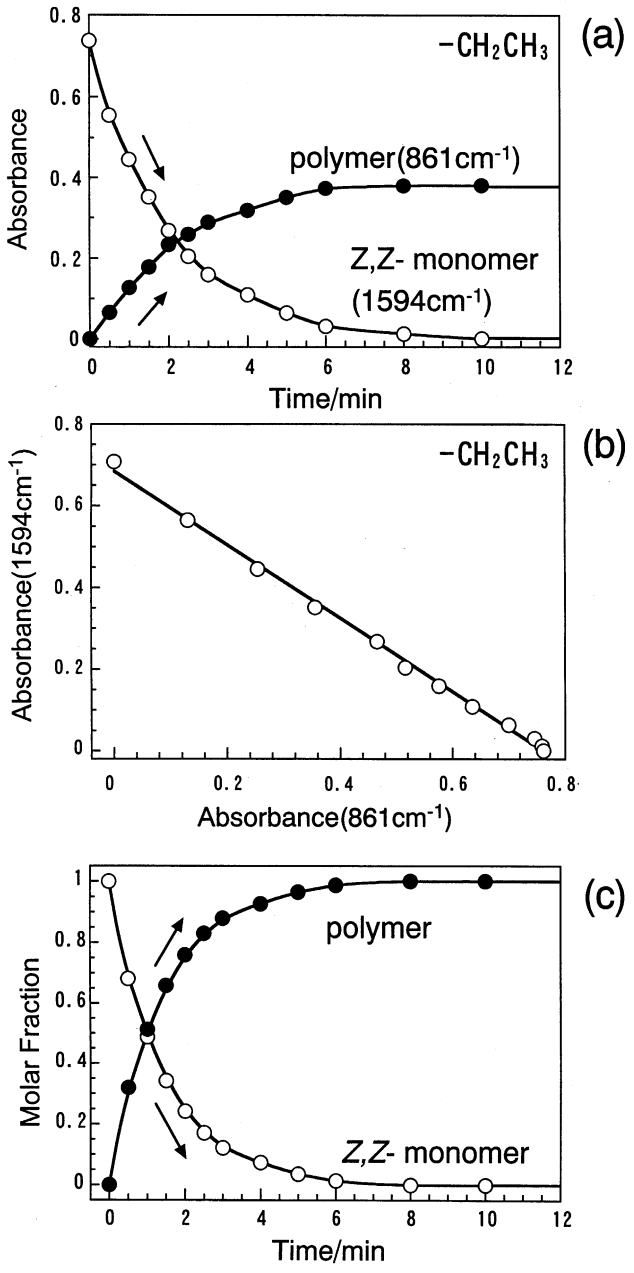

Fig. 7. Quantitative analysis of the infrared spectra of *Z,Z*-diethyl muconate. (a) Time dependence of the infrared absorbance evaluated for the monomer and the polymer, (b) a plot of the band intensity between the monomer (1594 cm^{-1}) and the polymer (861 cm^{-1}), and (c) the time dependence of the molar fractions estimated for the monomer and the polymer.

evaluated as follows

$$c_{\text{mono}} = 1/\{1 + (\epsilon_{ZZ}/\epsilon_{\text{poly}})[I_{\text{poly}}/[I_{ZZ} + (\epsilon_{ZZ}/\epsilon_{EE})I_{EE}]]\} \quad (13)$$

The c_{mono} thus obtained is a sum of the fraction of *Z,Z*- and *E,E*-isomers. The c_{ZZ} and c_{EE} can be evaluated as the following equations.

$$c_{ZZ}=c_{\text{mono}}/[1 + (I_{EE}/I_{ZZ})(\epsilon_{ZZ}/\epsilon_{EE})] \quad (14)$$

$$c_{EE} = c_{\text{mono}} - c_{ZZ} \quad (15)$$

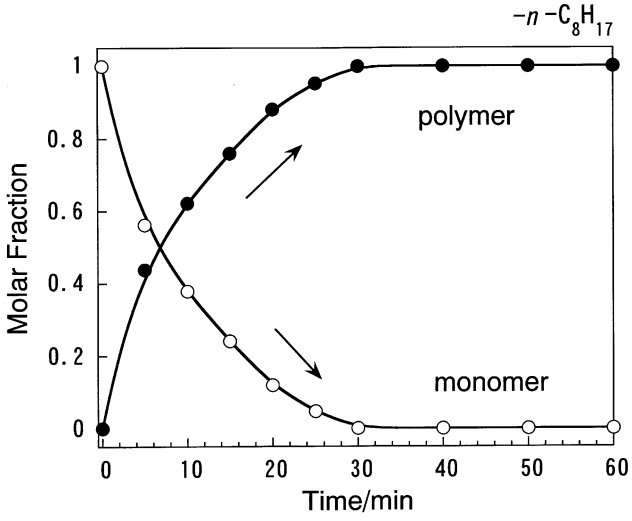

Fig. 8. Time dependence of the molar fractions estimated for the monomer and the polymer of bis-*n*-octyl *Z*,*Z*-muconate.

The actual application of these equations was made for the photo-reaction of dicyclohexyl *Z*,*Z*-muconate. Fig. 9(a) shows the intensity changes evaluated for the three types of the bands of *Z*,*Z*-monomer, *E*,*E*-monomer, and polymer. Fig. 9(b) shows the plot of $I_{ZZ} + (\epsilon_{ZZ}/\epsilon_{EE})I_{EE}$ against I_{poly}, where the intensities of the bands at 1710 cm^{-1} (*Z*,*Z*) and 1702 cm^{-1} (*E*,*E*) were used for the I_{mono} and the intensity of 1730 cm^{-1} band for I_{poly}. The plot is fitted with a straight line, indicating the reasonableness of the treatment. The slope $\epsilon_{ZZ}/\epsilon_{poly}$ was evaluated as 1.77. From Eqs. (14) and (15) the time dependence of each component is evaluated as shown in Fig. 9(c).

4. Evaluation of relative reactivity

The reaction order is estimated from the time dependence of the molar fraction. For all the reactions shown in Table 2, the logarithm of the fraction was found to be proportional to the first order of time as shown in Fig. 10, where the two examples of the diethyl and dicyclohexyl cases are illustrated. This result indicates these reactions to be the first-order reaction

$$\ln c_i = -kt \qquad (16)$$

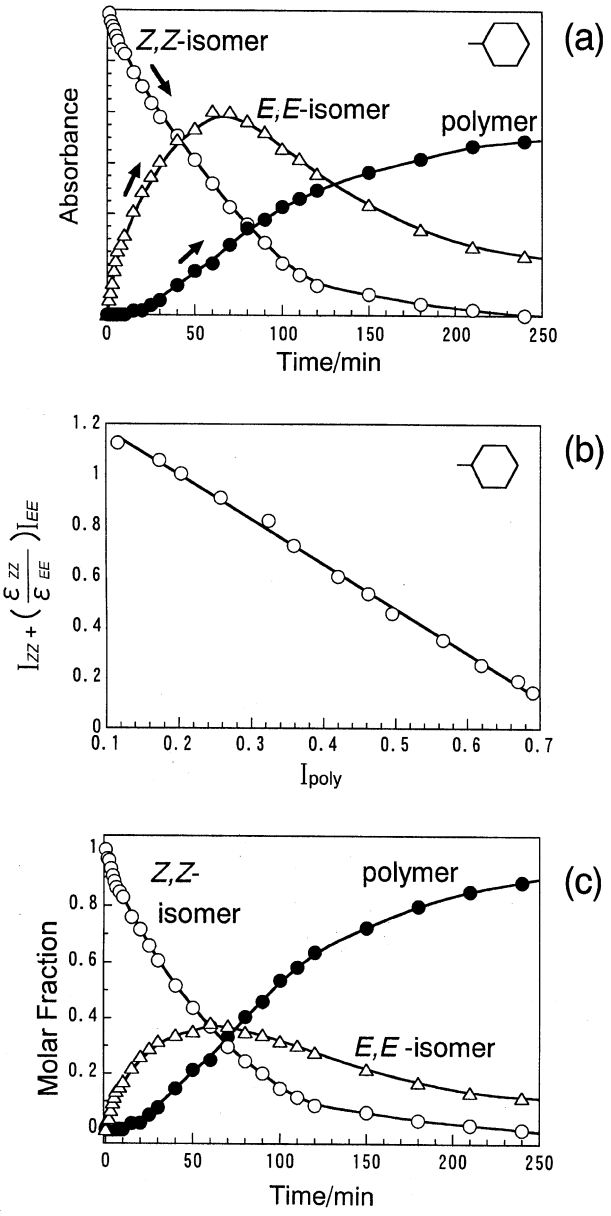

Fig. 9. Quantitative analysis of the infrared spectra of dicyclohexyl *Z*,*Z*-muconate. (a) Time dependence of the infrared absorbances evaluated for the *Z*,*Z*- and *E*,*E*-isomers and the polymer, (b) a plot of the band intensity between the monomer (sum of *Z*,*Z*- and *E*,*E*-species) and the polymer, and (c) the time dependence of the molar fractions estimated for the *Z*,*Z*- and *E*,*E*-monomers and the polymer.

Table 3
Rate constants *k* (min^{-1}) of the photo-induced solid-state reactions of various dialkyl *Z*,*Z*-muconates. (The list is made only for the reaction of *Z*,*Z*-monomer → tritactic polymer and the 2-step reaction of *Z*,*Z*-monomer → *E*,*E*-monome → atactic polymer. The reaction rate of *E*,*E*-monomer → atactic polymer starting from the original *E*,*E*-monomer is referred to in Table 4)

Side group R	*Z*,*Z* → tritactic polymer	*Z*,*Z* → *E*,*E* isomer	*E*,*E* → atactic polymer
$-CH_2CH_3$	0.703	–	–
Cyclohexyl	–	0.021	0.014
Benzyl	–	0.110	0.008
$-CH_2CF_3$	–	0.420	0.041

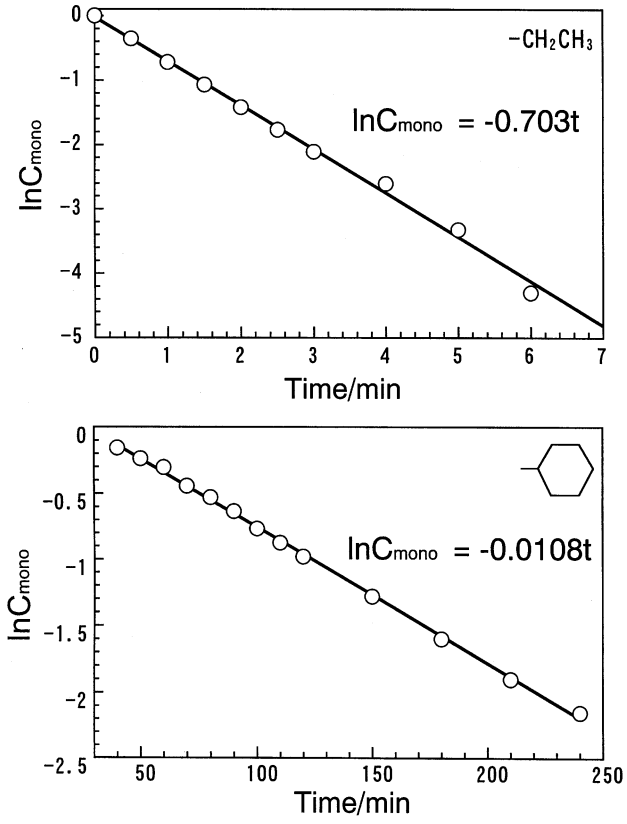

Fig. 10. Logarithmic plot of molar fraction against time. (a) diethyl *Z,Z*-muconate and (b) dicyclohexyl *Z,Z*-muconate.

where k is the rate constant. The thus estimated k values are listed in Table 3.

In the three-component reaction system, we need to obtain the rate constants of the individual reaction path. The possible reaction paths are illustrated in Fig. 11. Here we assume the two reaction paths. One is the reaction of *Z,Z*-isomer → *E,E*-isomer → atactic polymer. Another reaction path is *Z,Z*-monomer → atactic polymer. The reaction equations are developed in the following way

$$dc_{EE}/dt = k_1 c_{ZZ} - k_2 c_{EE} \tag{17}$$

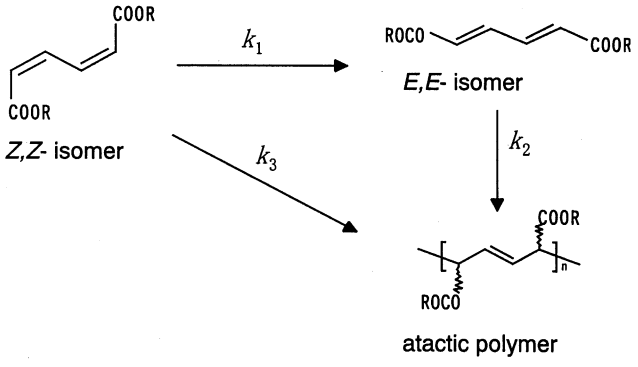

Fig. 11. Possible reaction paths expected for the dibenzyl and dicyclohexyl *Z,Z*-muconates.

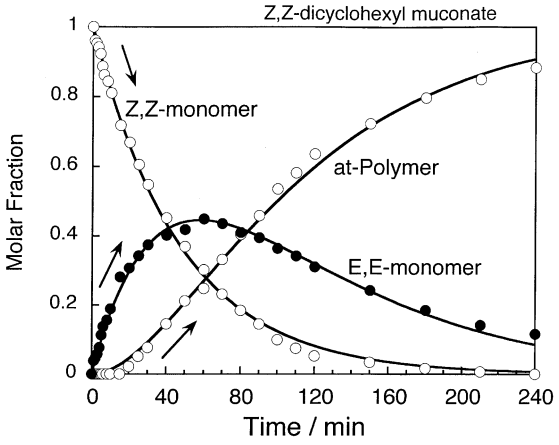

Fig. 12. Time dependence of the molar fractions evaluated for dicyclohexyl *Z,Z*-muconate. The open circles indicate the experimental data and the solid curves are the results of the curve fitting based on the equations developed for the three-component system (refer to the text).

$$dc_{ZZ}/dt = -k_1 c_{ZZ} - k_3 c_{ZZ} \tag{18}$$

$$dc_{poly}/dt = k_2 c_{EE} + k_3 c_{ZZ} \tag{19}$$

Eq. (18) can be solved as shown below, where the initial condition of '$c_{ZZ} = 1$ at $t = 0$' was used.

$$c_{ZZ} = \exp[-(k_1 + k_3)t] \tag{20}$$

From Eqs. (17) and (20), the c_{EE} can be obtained as follows.

$$c_{EE} = [k_1/(k_1 - k_2 + k_3)]\{\exp(-k_2 t) - \exp[-(k_1 + k_3)t]\} \tag{21}$$

Fig. 12 shows an example of the curve fittings made for the time dependencies of the molar fractions evaluated for *Z,Z*-dicyclohexyl muconate. The fittings are quite well and the rate constants k_1, k_2, and k_3 were evaluated as follows.

$$k_1 = 0.021, k_2 = 0.014, \text{ and } k_3 = 0.000$$

The constant k_3, which corresponds to the reaction of *Z,Z*-monomer → atactic polymer, is almost zero and can be neglected. In Table 3 are listed the values of k_1 and k_2 thus obtained. On the other hand, by plotting the logarithm of molar fractions against time, the rate constants of the *Z,Z* → *E,E* isomerization and the *E,E*-monomer → polymer reaction can be evaluated as 0.021 and 0.011 (Fig. 10) respectively. These values are in good agreement with k_1 and k_2, respectively, within the experimental errors, because the contribution of k_3 can be neglected as stated above. The rate constants were also evaluated by using the data in the early stage of the reaction, where the system could be treated as the two-component system (*Z,Z* → *E,E* isomerization). The rate constant was 0.021, almost the same with the above k_1. As stated above, the later stage of the reaction was treated by assuming the two-components system consisting of the monomer (*ZZ* + *EE*) and polymer. The corresponding rate constant was evaluated to be 0.011.

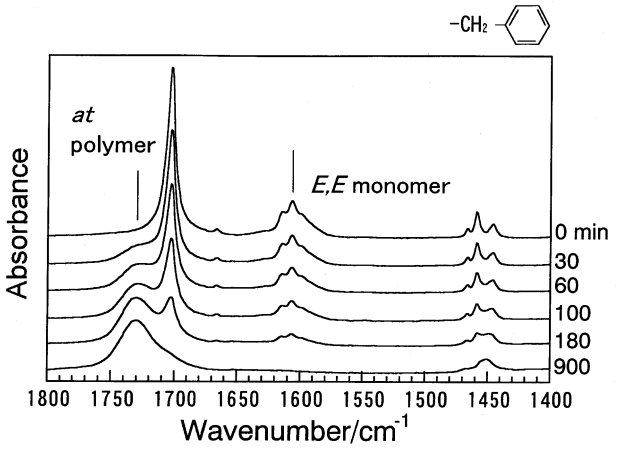

Fig. 13. UV irradiation time dependence of infrared spectra measured for dibenzyl *E*,*E*-muconate sample at room temperature.

Since the contribution of the reaction path of *Z*,*Z*-monomer → atactic polymer could be neglected because of $k_3 = 0$, the evaluated rate constant can be assumed as k_2 and a good agreement can be seen.

The similar data treatment was made also for the case of dibenzyl *Z*,*Z*-muconate. The results of the curve fittings were as follows

$$k_1 = 0.110, k_2 = 0.008, \text{ and } k_3 = 0.000$$

The k_3 is zero similarly to the case of dicyclohexyl *Z*,*Z*-muconate, meaning essentially the same reaction path with that of dicyclohexyl *Z*,*Z*-muconate.

As one method to check the reasonableness of these rate constants, we investigated the reaction of *E*,*E*-monomer to atactic polymer by starting from the separately synthesized *E*,*E*-monomer. Fig. 13 shows the infrared spectral change of dibenzyl *E*,*E*-muconate. The intensity of C=O stretching band at 1705 cm^{-1} decreased and the band of atactic polymer at 1730 cm^{-1} increased the intensity. No *Z*,*Z*-isomer band (1710 cm^{-1}) was observed during the reaction. The final product after UV irradiation for 900 min was found to give the same IR spectra to those of the atactic polymer obtained from the photo-irradiated *Z*,*Z*-isomer. The reaction rate of this polymerization process was evaluated with an assumption of the two-component analysis. The obtained rate constant 0.009 was found to be essentially the same as the k_2 value 0.008 evaluated from the corresponding reaction stage in the above-mentioned three-component system starting from the *Z*,*Z*-monomer. In this way the reaction of *E*,*E*-monomer → atactic polymer was found to be essentially identical in either case, starting from *Z*,*Z*-monomer and *E*,*E*-monomer.

The rate constant of *E*,*E*-monomer → atactic polymer reaction was investigated also for the other type of muconate with side group of ethyl. The obtained rate constant is compared with those of the corresponding *Z*,*Z*-monomer → polymer reaction as listed in Table 4. In the case of diethyl muconate, the *Z*,*Z*-monomer reacts to stereoregular polymer with quite high rate constant but the *E*,*E*-monomer reacts to atactic polymer at a rate an order of magnitude lower. In the case of dibenzyl muconate, the reaction from the *Z*,*Z*-monomer to atactic polymer does not occur actually, while the *E*,*E*-monomer changes to atactic polymer at a relatively high rate, although this rate is overwhelmingly lower than that of *E*,*E*-diethyl muconate. A similar situation can be seen also for dicyclohexyl muconate. In this way the reaction rate is quite different depending on the type of muconate compound.

Table 4
Rate constants of the polymerization reactions of *Z*,*Z* and *E*,*E*-muconates

Side group R	Configuration	Reaction	k (min^{-1})
-CH_2CH_3	*Z*,*Z*	→ tritactic polymer	0.703[a]
	E,*E*	→ atactic polymer	0.068[a]
Benzyl	*Z*,*Z*	→ atactic polymer	0.000[b]
	E,*E*	→ atactic polymer	0.009[c]
Cyclohexyl	*Z*,*Z*	→ atactic polymer	0.000[b]
	E,*E*	→ atactic polymer	0.014[d]
-*n*-C_8H_{17}	*Z*,*Z*	→ atactic polymer	0.112[a]
-CH_2CCl_3	*Z*, *Z*	→ atactic polymer	0.009[a]

[a] Obtained from the infrared date taken for the *E*,*E*- or *Z*,*Z*-monomer.
[b] The evaluated rate constant was quoted from k_3 (refer to the text).
[c] Obtained from the infrared date taken for the *E*,*E*-monomer. This value is in good agreement with k_2 (0.008) estimated in the text.
[d] The evaluated rate constant was quoted from k_2 (refer to the text).

5. Reactivity of monomers with different side groups

As seen in Tables 3 and 4, the topochemical reaction of *Z*,*Z*- and *E*,*E*-muconates is dependent on the type of the side group. The topotactic polymerization of *Z*,*Z*-EMU occurs at the rate 10–100 times faster than the *Z*,*Z* → *E*,*E* isomerization reaction and the monomer → atactic polymer reaction. In order to understand these processes, we need to know the packing of the initial monomer molecules and to relate them to solid-state reactivity. We carried out the X-ray structure analysis of these compounds by using the rapid-scan-type CCD camera system, which was used because the incident X-ray beams induced the photochemical reaction during the collection of X-ray reflection data. The details of the structural analysis procedure were reported in a separate paper [28]. The structural information obtained for a series of *Z*,*Z*-muconate compounds listed in Table 5 will be used for the discussion. As shown in Fig. 2, all of these compounds form a columnar structure. The carbon-to-carbon distance between the butadiene groups of the neighboring monomer molecules is almost the same for the compounds as listed in Table 5. The tilting angle of the molecular axis from the columnar axis is another important parameter. But, as seen in Table 5, it does not also serve effectively as a good measure of the reactivity.

In the polymerization reaction of these butadiene compounds the degree of overlap of the π-electron orbitals

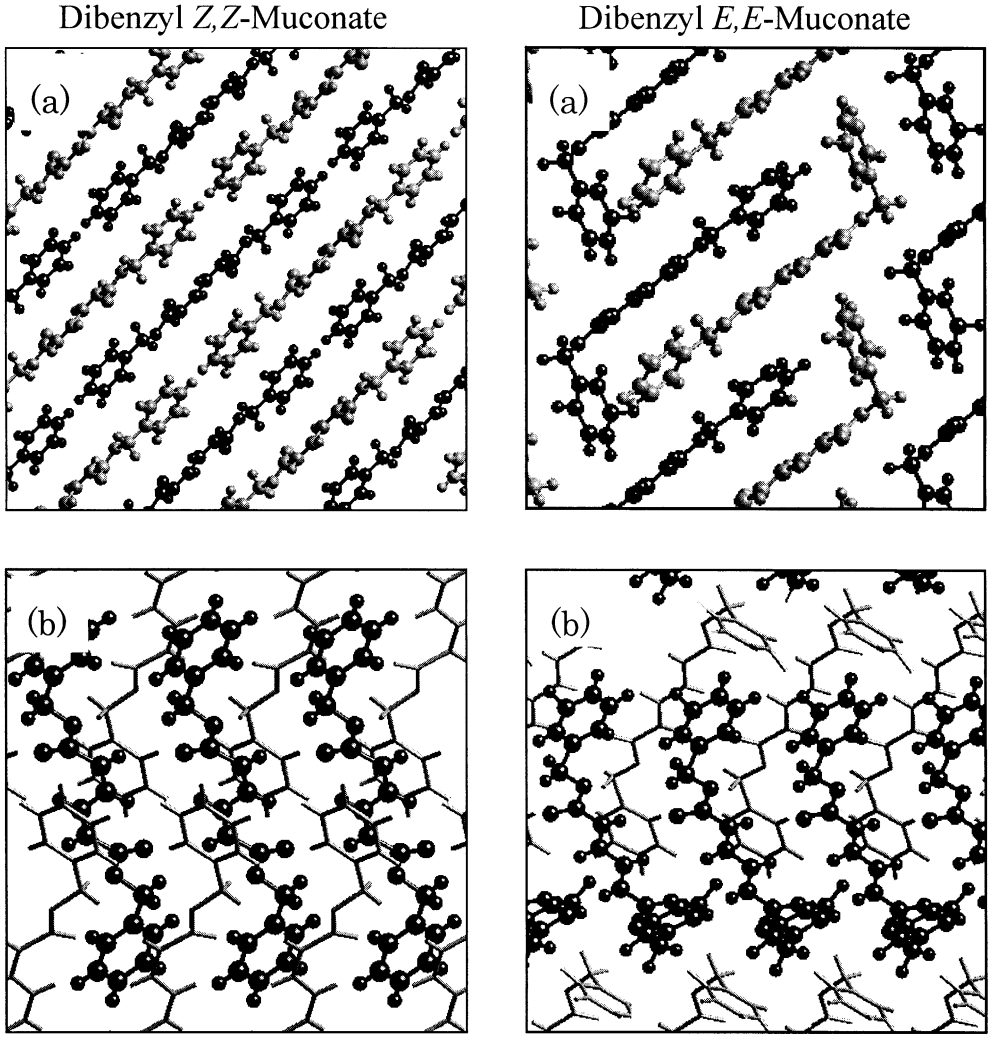

Fig. 14. Comparison of the molecular shape and the packing structure between the *Z,Z*- and *E,E*-dibenzyl muconate crystals. (a) Packing structure and (b) molecular conformation.

between the neighboring butadiene groups is considered to be one of the most important factors. This overlap was calculated as seen in Table 5. In this calculation the π-electron cloud was approximated as a box of a proper size and the volume of the overlapping part between the two adjacent boxes was calculated. The details of the calculation procedure will be reported elsewhere. Of course this overlap volume is only a rough and qualitative measure to know the tendency of overlap of the π-electron orbitals. That is, the value is only relative but does not have any absolute physical meaning. As shown in Table 5, the π-electron overlap is the largest for the topotactic polymerization reaction of *Z,Z*-EMU, about 21 Å^3. The compound with the overlapping volume of about 16 Å^3 ($R = CH_2CCl_3$) shows the polymerization reaction to give the atactic polymer product. The compounds undergoing the *Z,Z*- to

Table 5
Reaction rates and structural parameters of *Z,Z*-muconate

Side group R	Reaction	k (min^{-1})	d (Å)	ϕ (°)	Overlap (Å^3)
-CH_2CH_3	*Z,Z* isomer → tritactic polymer	0.703	3.76	48.1	20.7
-CH_2CCl_3	*Z,Z* isomer → atactic polymer	0.0084	4.02	38.4	16.5
Cyclohexyl	*Z,Z* → *E,E*	0.021	3.63	42.6	14.3
	(*E,E* → atactic polymer)	(0.014)			
Benzyl	*Z,Z* → *E,E*	0.11	6.42	78.2	6.2
	(*E,E* → atactic polymer)	(0.0078)			

E,*E*-isomerization reaction show overlap smaller than 14 Å^3 (R = cyclohexyl and benzyl). The small overlap of the orbitals might correspond to such a situation that the monomer molecule reacts in an isolated manner without any interference from the surrounding molecules. However, as for the reaction of *Z*,*Z*-monomer → atactic polymer, we can not give any explanation to the reason why the intermediate value of π-electron orbitals is related with this reaction. Further study is needed for this problem.

The step-wise reactions of *Z*,*Z*-dibenzyl muconate crystal are now considered. X-ray beam irradiation of *Z*,*Z*-species changes it into the *E,E*-species by an isomerization reaction. We analyzed the crystal structures of both the monomers of *Z*,*Z*- and *E*,*E*-species by the X-ray diffraction method [28]. The molecular shape is quite different between these two species. As seen in Fig. 14, the *Z*,*Z*-species takes a fully-extended conformation, while the *E*,*E*-species takes a conformation with one benzyl group bent from the molecular plane. When the X-ray beam irradiates the *Z*,*Z*-monomer, one benzyl group protrudes from the molecular plane by the change in the butadiene part from *Z*,*Z* to *E*,*E*-configuration. This configurational change and the rotation of the benzyl group are considered to be possible owing to the small overlap of the π-electrons between the neighboring molecules along the column axis.

6. Conclusions

By carrying out the time-resolved FT–IR measurements, a series of dialkyl *Z*,*Z*-muconate crystals were found to show the various types of photo-induced reactions depending on the kinds of the side groups. These reactions are classified into the following three types.

1. *Z*,*Z*-monomer → tritactic polymer
2. *Z*,*Z*-monomer → *E*,*E*-monomer → atactic polymer
3. *Z*,*Z*-monomer → atactic polymer

The rate constants of these reactions were evaluated through the quantitative analysis of the infrared band intensities. The topotactic polymerization reaction of *Z*,*Z*-EMU [case (1)] has a very high rate constant compared with those of the isomerization reaction [case (2)] and the polymerization reaction [case (3)]. These differences in reaction behavior were interpreted qualitatively on the basis of the structures analyzed for the starting monomer crystals. A simple calculation was made for the evaluation of the degree of overlap between the π-electron orbitals of the neighboring butadiene groups along the columnar axis in order to learn the relation between the packing structure of monomer molecules and the reactivity. Some tendency can be obtained between the reactivity and the π-electron overlap: the largest overlap gives the rapid polymerization reaction of *Z*,*Z*-EMU crystal. Unfortunately, however, at the present stage we can not understand the mechanism of the photo-induced solid-state reactions of a series of muconates in a systematic way. The molecular orbital calculation of the crystal, for example, might provide an answer to this problem.

References

[1] Kohlshutter HZ. Anorg Allig Chem 1918;105:121.
[2] Schmidt GMJ. Pure Appl Chem 1971;27:647.
[3] Ramamurthy V, Venkatesan K. Chem Rev 1987;87:432.
[4] Cohen MD, Schmidt GMJ. J Chem Soc 1964;1964:1996.
[5] Cohen MD, Schmidt GMJ, Sonntag FI. J Chem Soc 1964;1964:2014.
[6] Bregman J, Osaki K, Schmidt GMJ, Sonntag FI. J Chem Soc 1964;1964:2021.
[7] Okamura S, Hayashi K, Kitanishi Y, Nishii M. Makromol Chem 1961;47:230.
[8] Chatani Y, Kitahama K, Uchida T, Tadokoro H, Hayashi K, Nishii M, Okamura S. J Macromol Sci 1968;2:567.
[9] Hasegawa M, Suzuki Y. J Polym Sci 1967;B5:813.
[10] Suzuki F, Suzuki Y, Nakanishi H. J Polym Sci Part A-1 1969;7:2319.
[11] Nakanishi H, Hasegawa M. J Polym Sci Part A-2 1972;10:1537.
[12] Wegner G. Z Naturforsch 1969;24b:824.
[13] Wegner G. Pure Appl. Chem 1977;47:443.
[14] Enkelmann V. Adv Polym Sci 1984;63:91.
[15] Cohen MD, Garito AF, Heeger AJ, MacDiarmid AG, Mikulski CM, Saran MS, Kleppinger J. J Am Chem Soc 1976;98:3844.
[16] Cheng K, Foxman BM. J Am Chem Soc 1977;99:8102.
[17] Matsumoto A, Matsumura T, Aoki S. J Chem Soc Chem Commun 1994;1994:1389.
[18] Matsumoto A, Odani T, Chikada M, Sada K, Miyata M. J Am Chem Soc 1999;121:11122.
[19] Matsumoto A, Odani T. Polym J 1999;31:717.
[20] Matsumoto A, Odani T, Sada K, Miyata M, Tashiro K. Nature 2000;405:328.
[21] Matsumoto A, Matsumura T, Aoki S. Macromolecules 1996;29:243.
[22] Matsumoto A, Yokoi K, Aoki S, Tashiro K, Kobayashi M. Macromolecules 1998;31:2129.
[23] Matsumoto A, Yokoi K, Aoki S. Polym J 1998;30:361.
[24] Tashiro K, Kamae T, Kobayashi M, Matsumoto A, Yokoi K, Aoki S. Macromolecules 1999;32:2449.
[25] Tashiro K, Zadorin AN, Saragai S, Kamae T, Matsumoto A, Yokoi K, Aoki S. Macromolecules 1999;32:7946.
[26] Matsumoto A, Yokoi K, Aoki S, Tashiro K, Kamae T. Polym Prepr, Jpn 1998;47:142.
[27] Matyjaszawski K, editor. Controlled/living radical polymerization: progress in ATRP, NMP, and RAFT. Washington, DC: American Chemical Society, 2000.
[28] Tashiro K, Saragai S, Zadorin AN, Kamae T, Nakamoto S, Matsumoto A, Yokoi K, Aoki S. Polym Prepr, Jpn 1998;47:3863.